Upconverting nanovesicles for the activation of ruthenium anti-cancer prodrugs with red light

Askes, S.H.C.

CHAPTER 6

Temperature dependence of triplet-triplet annihilation upconversion in phospholipid membranes

Understanding the temperature dependency in photon-upconverting nano-systems is important to realize optimized upconversion applications. In this chapter, the temperature dependency of red-to-blue triplet-triplet annihilation upconversion in a variety of neutral PEGylated phospholipid membranes is reported. It appears that in these systems a delicate balance between lateral diffusion rate, annihilator aggregation, and sensitizer self-quenching and thermal deactivation leads to the maximization of the upconversion intensity near the main transition temperature of the membrane.

Sven H.C. Askes, Philip Brodie, Gilles Bruylants, and Sylvestre Bonnet. Manuscript in preparation.

6.1 Introduction

Light upconversion is the generation of high-energy photons from low-energy photons, for example the conversion of red light to blue light. Generating upconverted light can be achieved through various mechanisms and in different materials, such as two-photon absorption dyes, energy upconversion processes in rare-earth doped materials or nanoparticles, and triplet-triplet annihilation (TTA-UC) in solution and solid state materials. Among these principles, TTA-UC offers many advantages: it can occur at low excitation power (in the best cases even lower than 1 $mW.cm^{-2}$), it uses sensitizers having high molar absorptivity, and the obtained upconversion quantum yields may reach up to 14% in aqueous solution.[1] Since its popularization more than a decade ago,[2] TTA-UC has been used in many applications such as photocatalysis,[3] solar energy harvesting,[4] drug delivery and activation,[5] and luminescence bio-imaging.[1a, 6]

TTA-UC is based on the photophysical interplay of photosensitizer and annihilator chromophores (see Chapter 2, Figure 2.1).[7] The photosensitizer absorbs low energy light, after which intersystem crossing leads to a long-lived triplet state. The energy of this triplet state is transferred to the annihilator upon diffusional collision by means of triplet-triplet energy transfer (TTET); a succession of TTET leads to a concentration buildup of long-lived triplet-state annihilators. Two triplet state annihilators can then perform triplet-triplet annihilation upconversion, in which one of them departs with the energy of both to reach a high-energy singlet state. Finally, this singlet excited state returns to the ground state by emission of a high-energy photon, thus realizing light upconversion. TTA-UC has been demonstrated in an extensive assortment of organic, inorganic, and/or supramolecular materials,[1c, 8] as well as in nano or micro-sized particles.[9]

Among the various applications in the field of TTA-UC, there are some that are not operated at room temperature, such as bio-imaging and phototherapy. It is thus important to understand the temperature dependency of upconversion efficiency in order to optimize the use of TTA-UC. Because TTET and TTA occur *via* molecular contact, they are highly dependent on molecular diffusion; the efficiency of TTA-UC is generally greatly influenced by the fluidity and hence thermal responsiveness of the host material.[10] For many materials, a higher temperature leads to a higher fluidity, and therefore to higher TTA-UC efficiency. For example, green-to-blue TTA-UC in a rubbery polymer matrix

was only visible above the glass transition temperature of the material, above which the matrix becomes more fluid.[11] However, diffusion is not the only important factor. First of all, temperature-dependent chemical phenomena such as dye aggregation may affect upconversion as well: counter-intuitively, it was recently shown that at lower temperatures, mixed aggregation of sensitizer and annihilator molecules in diluted conditions resulted in higher TTA-UC efficiency.[12] It has also been shown that upconversion in gel matrices decreased at higher temperatures due to temperature-dependent disassembly of the host-material.[8c] Overall, understanding the temperature-dependence of all chemical and physical properties of a given medium, is necessary for optimizing upconversion.

Our group recently demonstrated that green-to-blue and red-to-blue TTA-UC can be realized in the phospholipid membrane of neutral PEGylated liposomes composed of 1,2-dimyristoyl-sn-glycero-3-phosphocholine (DMPC). This knowledge was later used for the activation of photoactivatable chemotherapeutic agents in the photodynamic window.[5] In our initial studies it was reported that the upconversion intensity was reversibly affected by changes in temperature. [5b] Upon heating the sample from 15 to 25 °C the upconversion intensity increased significantly, which we interpreted as a consequence of the gel-to-liquid crystalline phase transition temperature (T_m) of the DMPC lipid bilayer. Upon raising the temperature above T_m the molecular diffusion of the dyes in the membrane is expected to increase greatly, which should lead to higher TTET and TTA rates, and thus higher TTA-UC efficiencies. In this work, we evaluate the general applicability of this hypothesis by systematically investigating the temperature dependency of TTA-UC in neutral PEGylated liposomes, using different lipids with different T_m.

6.2 Results and discussion

Neutral PEGylated liposome dispersions were prepared in phosphate buffered saline (PBS) by hydration and extrusion of lipid films containing five different neutral phosphatidylcholines, *i.e.* 1,2-dioleyl-*sn*-glycero-3-phosphocholine (DOPC), 1,2-dilaureyl-*sn*-glycero-3-phosphocholine (DLPC), 1,2-dimyristoyl-*sn*-glycero-3-phosphocholine (DMPC), 1,2-dipentadecanoyl-*sn*-glycero-3-phosphocholine (DPDPC), and 1,2-dipalmitoyl-*sn*-glycero-3-phosphocholine (DPPC), and in presence of 4 mol% of sodium N-(carbonyl-methoxypolyethylene glycol-2000)-1,2-distearoyl-*sn*-glycero-3-

phosphoethanolamine (DSPE-MPEG-2000, see Figure 6.1). Addition of DSPE-MPEG-2000 is a well-known strategy to prevent liposome aggregation and fusion. The lipid composition of liposome samples **O**, **L**, **M**, **PD**, and **P** is shown in Table 6.1. A well-investigated red-to-blue TTA-UC dye couple consisting of palladium tetraphenyltetrabenzoporphyrin (**1**) and perylene (**2**, see Figure 6.1) was selected for incorporation in the liposomes. Samples containing these dyes, *i.e.* **O12**, **L12**, **M12**, **PD12**, and **P12** (defined in Table 6.1), were prepared following an identical procedure. The hydrodynamic diameters (z-ave = 135 ± 5 nm) and polydispersity indices (PDI = 0.09 ± 0.02), as measured by dynamic light scattering (DLS), were found to be very similar regardless of the lipid type or dye functionalization.

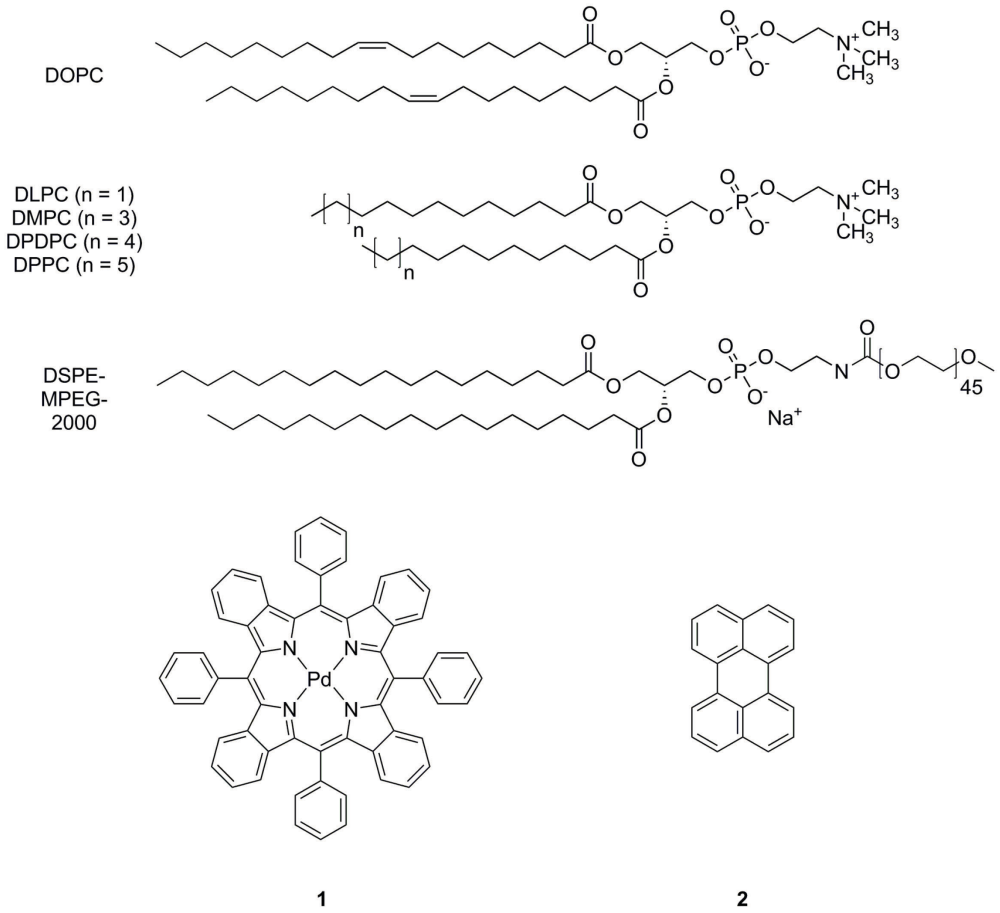

*Figure 6.1. Chemical structures of DOPC, DLPC, DMPC, DPDPC, DPPC, DSPE-MPEG-2000, palladium tetraphenyltetrabenzoporphyrin (**1**), and perylene (**2**).*

Table 6.1. Lipid formulations of the PEGylated phosphatidylcholine liposomes used in this work, and their physical characterization by dynamic light scattering (with z-ave as hydrodynamic diameter and PDI as polydispersity index) and differential scanning calorimetry. DSC measurements were performed with a scanning rate of 1 °C.min^{-1} at 3 atm. pressure.

Sample	Lipid[a]	[1] (μM)	[2] (μM)	z-ave (nm)	PDI	T_m (lit. value)[13] (°C)[b]	ΔH (lit. value)[13] (kJ.mol^{-1})[b]
O	DOPC			139	0.11	- (−18.2)	- (35.5)
O1	DOPC	2.5					
O1'	DOPC	25					
O2	DOPC		25				
O12	DOPC	2.5	25	135	0.11	-	-
L	DLPC			127	0.11	- (−2.1)	- (7.5)
L12	DLPC	2.5	25	134	0.12	-	-
M	DMPC			132	0.07	25.0 (23.9)	27.7 (29.3)
M1	DMPC	2.5					
M2	DMPC		25				
M12	DMPC	2.5	25	134	0.09	24.9	26.6
PD	DPDPC			132	0.09	34.9 (34.7)	33.6 (32.7)
PD12	DPDPC	2.5	25	140	0.07	34.6	32.0
P	DPPC			140	0.08	42.4 (41.4)	40.1 (36.8)
P12	DPPC	2.5	25	137	0.11	42.1	38.7

[a] All liposomes were prepared with 5.0 mM lipid and 0.20 mM DSPE-mPEG-2000.[b] T_m is defined as the main transition temperature of the bilayer, and ΔH as the molar enthalpy change of the phase transition (the enthalpy change of the pretransition is included, in case there is one). Literature T_m and ΔH values given for the pure phospholipids.

It is well known that phase changes of phospholipid membranes greatly influence the two-dimensional translational molecular diffusion coefficient (D_T in μm^2.s^{-1}) of membrane solutes. Therefore, the gel-to-liquid phase transition temperature (T_m) and the total enthalpy change of the phase transition (ΔH) were measured for samples based on DMPC, DPDPC, and DPPC using differential scanning calorimetry (DSC, see Table 6.1 and Figure 6.2b). T_m and ΔH for dye-free PEGylated liposomes **M**, **PD**, and **P** were found to be very close to literature values for PEG-free liposomes, *i.e.* the PEG groups do not significantly influence the phase transition at these concentrations. Upon functionalization of the PEGylated liposomes with compounds **1** and **2**, a small decrease in the main transition peak height was observed, but the main features of the thermogram remained. These results indicate that for liposome samples **M12**, **PD12**, and **P12**, compounds **1** and **2** were indeed buried in the lipid bilayer, and that their presence only minimally perturbed the physical properties of the membranes. No transitions were found between 5 and 50 °C for samples **O**, **O12**, **L**, and **L12**, because T_m for pure DOPC and DLPC are reported to be below the freezing point of water.[13]

Next, UV-vis absorption and emission spectroscopy was performed on samples **O12**, **L12**, **M12**, **PD12**, and **P12** at 20 °C in presence of 0.3 M sodium

sulfite for chemical deoxygenation, see Figure 6.2.[5a, 14] The absorption spectra show the superposition of the characteristic peaks of **1** at 440 and 630 nm and the vibronically structured band of **2** from 350 – 450 nm.[5b] Upon irradiation with 630 nm laser light (10 mW, 80 mW.cm^{-2}), phosphorescence of **1** at 800 nm and upconversion emission of **2** at 474 nm were observed for each sample. The emission stability at 20 °C was tested for each formulation by continuously irradiating for one hour and collecting emission spectra. All samples exhibited good emission stability during this period, see Figure S.V.1.

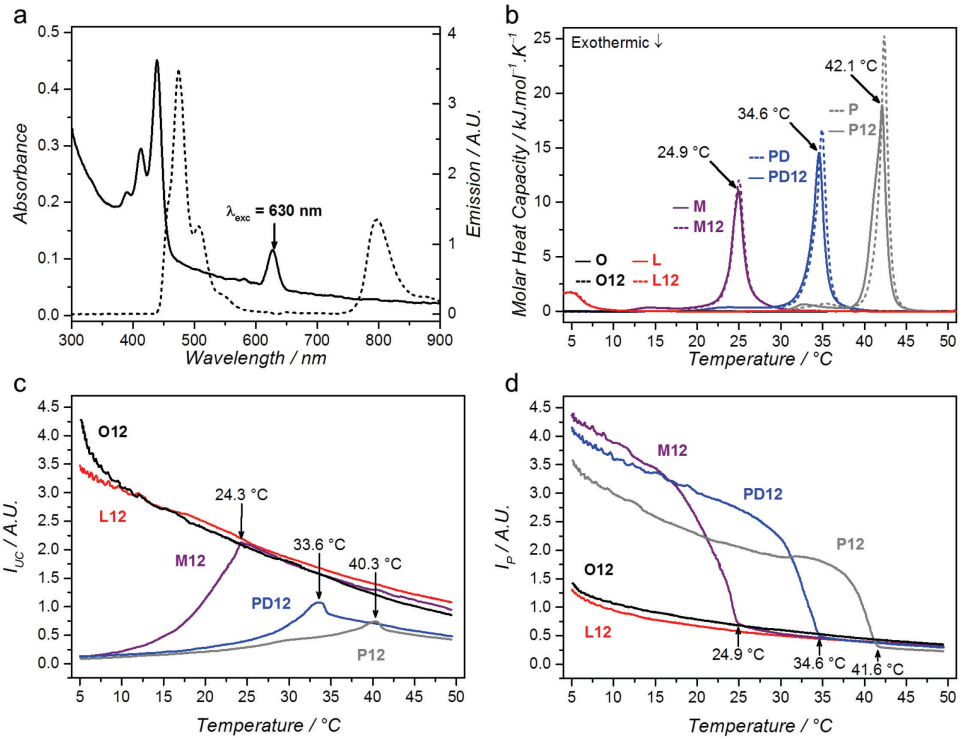

*Figure 6.2. (Photo)physical characterization of upconverting liposomes. a) Typical absorption (solid, left axis) and emission spectrum (dashed, right axis, λ_{exc} = 630 nm, intensity 80 mW.cm^{-2}) of **L12** liposomes ([DLPC] = 1.0 mM) at 20 °C in 0.3 M sodium sulfite PBS under air. b) Differential scanning calorimetry thermograms between 5 °C and 50 °C of liposomes with TTA-UC dyes (**O12**, **L12**, **M12**, **PD12**, and **P12**, solid) or without (**O**, **L**, **M**, **PD**, **P**, dashed). Arrows indicate T_m of the dyed liposomes, where applicable. Measurements were performed in heating mode with a scanning rate of 1 °C.min^{-1} at 3 atm. pressure. c & d) Temperature evolution of the upconversion intensity at 474 nm (c) and of the phosphorescence intensity (d) of **O12**, **L12**, **M12**, **PD12**, and **P12**. Samples were heated from 5 °C to 50 °C at a rate of 0.3 °C.min^{-1} while continuously irradiated with 80 mW.cm^{-2} 630 nm light.*

To investigate the temperature dependency of TTA-UC in **O12**, **L12**, **M12**, **PD12**, and **P12**, these samples were heated from 5 °C to 50 °C at a rate of 0.3

°C.min^{-1} while stirring, and upconversion spectra were continuously recorded. A submerged thermocouple registered the accurate temperature inside the solution. Figure 6.2 shows the evolution of the luminescence intensities at 800 nm (I_P) and 474 nm (I_{UC}) *vs.* temperature for each liposome formulation. For **O12** and **L12**, both phosphorescence and upconversion intensity gradually decreased with increasing temperature. For **M12**, **PD12**, and **P12**, I_{UC} increased up to 25, 35, and 42 °C, respectively, and then decreased gradually, whereas I_P decreased steeply up to 25, 35, and 42 °C, respectively, and then continued to decrease, but less steeply. When the samples were brought back from 50 °C to 5 °C, the initial emission spectra at 5 °C were obtained again in all cases except for **O12**, showing that bleaching did not occur and that the thermo-photophysical evolution is reversible (Figure S.V.2). For **O12**, we attribute this relative instability to the presence of the unsaturated bond, which might participate in undesired photochemical reactions. Interestingly, for **M12**, **PD12**, and **P12**, the temperature values at which I_{UC} maximizes and I_P kinks are very close to the phase transition temperature of the bilayer (T_m) recorded with DSC.

The increase of I_{UC} when approaching T_m is easily explained: heating the liposomes above T_m greatly increases the membrane fluidity and thus increases the lateral diffusion coefficient (D_T) of membrane dyes, which in turn causes an increase in TTA-UC efficiency. For instance, the D_T for fluorescent probes in DMPC lipid bilayers has reported to increase from 0.01 μm^2.s^{-1} at 15 °C, to 6 μm^2.s^{-1} at 30 °C to 13 μm^2.s^{-1} at 50 °C.[13, 15] It is worth mentioning that for such DMPC bilayers, the foremost change in D_T (a three-order increase in magnitude) was found between 20 and 25 °C, and so the most considerable transition in TTA-UC efficiency was expected to occur in this temperature domain. This is indeed in accordance with our data for **M12**.[15] In absence of accurate literature data of D_T in DPDPC and DPPC across the full temperature range, we assume that the same explanation holds for the results obtained with **PD12** and **P12**. However, this rationale is clearly no longer valid above T_m: although D_T continues to increase (*vide supra*), I_{UC} decreased. Furthermore, for **O12** and **L12**, in absence of a phase transition between 5 and 50 °C, I_{UC} and I_P both decrease across the whole temperature range. It is thus clear that other photophysical phenomena must play a role in the temperature dependence of TTA-UC in lipid bilayers.

Therefore, the thermo-photophysical behavior of the isolated dyes was considered in DOPC, DMPC, and in toluene (Figure 6.3). First, the fluorescence

intensity of compound **2** (λ_{exc} = 420 nm, λ_{em} = 474 nm) was found to decrease by 10% in both DOPC liposomes and toluene when heated from 5 °C to 50 °C. This is most likely explained by a slightly increased thermal deactivation. In DMPC, the fluorescence intensity increased by 25% when heated from 5 °C to 30 °C, with the most sharp increase around 25 °C, and then decreased slightly again up to 50 °C. This observation is in agreement with the work of Khan *et al.* who reported that perylene tends to form staggered aggregates in the tightly packed gel membrane below T_m, which break apart in the more loosely packed liquid-crystalline state above T_m.[16] Since the fluorescence intensity is lower in presence of such aggregates, the TTA-UC efficiency is lower below T_m. Overall, dissociation of perylene aggregates gives an additional explanation for the increase of upconversion intensity up to T_m.

Secondly, the phosphorescence intensity of **1** (λ_{exc} = 630 nm, λ_{em} = 800 nm) was investigated under deoxygenated conditions. In toluene solution, roughly 50% of the phosphorescence intensity is lost upon going from 5 °C to 50 °C due to increased thermal deactivation. When the dye was inserted into DOPC or DMPC liposomes (**O1** and **M1**, respectively) about 70% phosphorescence intensity was lost upon going from 5 °C to 50 °C; the additional 20% loss of phosphorescence intensity with respect to the toluene sample may be due to increased dynamic self-quenching, because the molecules are much more confined in the lipid bilayer. The explanation of self-quenching is supported by the fact that for **M1**, the highest loss of phosphorescence is observed around the transition temperature, at which the fluidity of the membrane increases most rapidly and diffusion-based processes such as self-quenching are expected to have an increased effect. Overall, these results explain that the decrease of TTA-UC with rising temperature is most likely due to increased thermal deactivation and self-quenching of **1**.

Based on these data, we explain the typical maximization of I_{UC} around T_m in lipid bilayers that have a transition temperature between 5 and 50 °C as follows. On the one hand, the increase in photosensitizer quenching as a function of temperature is rather linear (Figure 6.3). On the other hand, the temperature dependence of D_T has been described in literature as sigmoidal, with three-orders of magnitude increase when approaching T_m, and flattening directly after T_m.[15] In other words, upon approaching T_m the membrane becomes fluid rather quickly, but once it reaches the liquid crystalline state the fluidity changes negligibly. Therefore, above T_m the effect of the only minor increase in lateral diffusion coefficient on the upconversion efficiency is

completely outcompeted by the increased quenching of the photosensitizer. Furthermore, the dissociation of annihilator aggregates results in a rather abrupt and significant increase in fluorescence around T_m as well (Figure 6.3a). It is thus concluded that the combination of these three temperature-dependent phenomena results in the maxima that were observed in the I_{UC} *versus* temperature curve at 24, 34, and 40 °C for samples **M12**, **PD12**, and **P12**, respectively (Figure 6.2c).

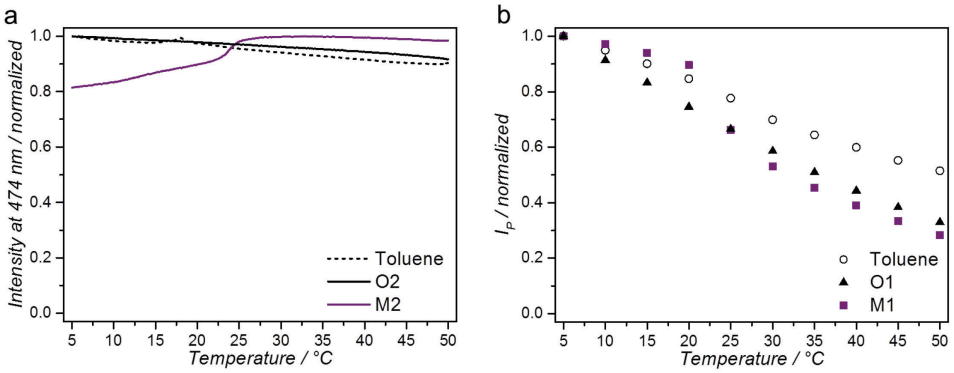

*Figure 6.3. Temperature-dependent emission spectroscopy of compounds **2** or **1** in toluene, DMPC liposomes, or DOPC liposomes. a) Normalized fluorescence intensity at 474 nm of compound **2** in toluene (dashed, 20 μM), **M2** liposomes (purple, [DMPC] = 1 mM), or **O2** liposomes (black, [DOPC] = 1 mM) as a function of temperature. λ_{exc} = 420 nm, 0.7 mW (6 mW.cm^{-2}). b) Temperature variation of the normalized phosphorescence intensity at 800 nm in 5 °C intervals for compound **1** in toluene under argon (open circles) and for liposomes **O1** (black triangles, [DOPC] = 1 mM) or **M1** (purple squares, [DMPC] = 1 mM) prepared in PBS with 0.3 M sodium sulfite. λ_{exc} = 630 nm, 10 mW (80 mW.cm^{-2}).*

Finally, for the biological application of these upconverting liposomes in bio-imaging or phototherapy, it would be beneficial to achieve the highest upconversion intensity at human body temperature (37 °C). From our results, it is evident that the systems **O12**, **L12**, and **M12** achieve identical upconversion intensities at 37 °C, while **PD12** and **P12** exhibit inferior intensities. We cannot offer any explanation why I_{UC} is lower in **PD12** and **P12**. Altogether, the results suggest that even though I_{UC} maximizes around T_m (for **M12**, **PD12**, and **P12**), choosing a lipid with a T_m near 37 °C does not result in an optimized upconverting liposome formulation. Finally, considering that little has been reported about the biocompatibility of DLPC,[I] we conclude that

[I] In preliminary experiments, A549 lung carcinoma cells were incubated with **L12** liposomes ([DLPC] = 0.5 mM) for 4 h, which resulted in 100% cell death (data not shown).

O12 and **M12** upconverting liposomes are the most promising for biological applications.

6.3 Conclusion

The temperature dependence of red-to-blue TTA-UC was studied in PEGylated liposomes with PC lipids with different lipophilic chain lengths and transition temperatures, and it was found that the upconversion intensity maximizes around T_m. Three major effects contribute to this temperature dependency: (1) an increase in lipid bilayer fluidity above T_m results in higher diffusion rates and thus higher rates of TTET and TTA, (2) dissociation of perylene aggregates when approaching T_m results in higher annihilator emission intensity, and (3) higher thermal deactivation and self-quenching rates of the photosensitizer at higher temperatures lead to a lower TTET rate and lower upconversion intensity beyond T_m. Measuring the point at which I_{UC} maximizes may be exploited for probing the transition temperature of phospholipid membranes. Furthermore, for TTA-UC applications that require high performance at elevated temperatures, the results underline the importance of selecting photosensitizers that are minimally affected by temperature. Finally, all liposome formulations were efficient in upconversion at biological temperature, which underlines that liposomes are versatile platforms for upconversion bio-imaging and photopharmaceutical applications. The phospholipid can be freely chosen to further optimize the liposomal formulation in terms of medium stability, biocompatibility, clearance from the bloodstream, and surface functionalization.

6.4 Experimental

6.4.1 General

Palladium tetraphenyltetrabenzoporphyrin (**1**) was purchased from Bio-Connect (Huissen, The Netherlands). Perylene (**2**) was purchased from Sigma-Aldrich Chemie BV (Zwijndrecht, The Netherlands). All lipids were purchased from either Lipoid GmbH (Ludwigshafen, Germany) or Avanti Polar Lipids (Alabaster, AL, USA) and stored at −18 °C. Dulbecco's phosphate buffered saline (DPBS) was purchased from Sigma Aldrich and had a formulation of 8 $g.L^{-1}$ NaCl, 0.2 $g.L^{-1}$ KCl, 0.2 $g.L^{-1}$ KH_2PO_4, and 1.15 $g.L^{-1}$ K_2HPO_4 with a *pH* of 7.1 − 7.5.

6.4.2 Liposome assembly

All liposome formulations were prepared by the classical hydration-extrusion method. As an example, the preparation of **O12** is described here. Aliquots of chloroform stock solutions containing the liposome constituents were added together in a flask to obtain a solution with 5.0 µmol DOPC, 0.20 µmol DSPE-MPEG-2000, 2.5 nmol compound **1**, and 25 nmol compound **2**. The organic solvent was removed by rotary evaporation and subsequently under high vacuum

for at least 30 minutes to create a lipid film. 1.0 mL DPBS buffer, with or without 0.3 M sodium sulfite, was added and the lipid film was hydrated by 4 cycles of freezing the flask in liquid nitrogen and thawing in warm water (50 °C). The resulting dispersion was extruded through a Whatman Nuclepore 0.2 μm polycarbonate filter at 40 − 50 °C at least 11 times using a mini-extruder from Avanti Polar Lipids, Inc. (Alabaster, Alabama, USA). The number of extrusions was always odd to prevent any unextruded material ending up in the final liposome sample. The extrusion filter remained practically colorless after extrusion, suggesting near-complete inclusion of the chromophoric compounds in the lipid bilayer. Liposomes were stored in the dark at 4 °C and used within 7 days. The average liposome size and polydispersity index were measured with a Malvern Instruments Zetasizer Nano-S machine, operating with a wavelength of 632 nm.

6.4.3 Differential Scanning Calorimetry

Differential scanning calorimetry (DSC) was performed on a TA Instruments (DE, USA) nano-DSC III instrument in the range of 5 °C to 50 °C with a scanning rate of 1 °C.min^{-1} at 3 atm. The capillary cell (V = 300 μL) was filled with the liposome solution (lipid bulk concentration of 5 mM), and the reference cell was filled with PBS buffer solution. A blank measurement was performed with PBS buffer. The liposome dispersions were degassed for 10 − 15 minutes prior to measurement on a Nalgene degassing station. For each sample, at least two cycles of heating and cooling were performed with 10 minutes of thermal equilibration between the ramps. The machine was cleaned beforehand with 50% formic acid and rinsed thoroughly with Milli-Q water. The thermograms were processed and analyzed using NanoAnalyze software from TA Instruments.

6.4.4 Absorption and emission spectroscopy

Absorption and emission spectroscopy was conducted in a custom-built setup (Figure S.V.3). All optical parts were connected with FC-UVxxx-2 (xxx = 200, 400, 600) optical fibers from Avantes (Apeldoorn, The Netherlands), with a diameter of 200-600 μm, respectively, and that were suitable for the UV-Vis range (200-800 nm). Typically, 2.25 mL of sample was placed in a 111-OS macro fluorescence cuvette from Hellma in a CUV-UV/VIS-TC temperature-controlled cuvette holder with stirring from Avantes. Deoxygenated toluene samples were prepared in a glovebox in a sealed fluorescence cuvette. The cuvette holder temperature was controlled with a TC-125 controller and T-app computer software from Quantum Northwest (Liberty Lake, WA, USA), while the sample temperature was measured with an Omega RDXL4SD thermometer with a K-type probe submerged in the sample. The sample was excited with a collimated 630 nm laser light beam (4 mm beam diameter) from a Diomed 630 nm PDT laser. The 630 nm light was filtered through a FB630-10, 630 nm band pass filter (Thorlabs, Dachau/Munich, Germany) put between the laser and the sample. The excitation power was controlled using the laser control in combination with a NDL-25C-4 variable neutral density filter (Thorlabs), and measured using a S310C thermal sensor connected to a PM100USB power meter (Thorlabs). For regular measurements, the excitation power was set at a power of 10 mW (80 mW.cm^{-2}). UV-Vis absorption spectra were measured using an Avalight-DHc halogen-deuterium lamp (Avantes) as light source and a 2048L StarLine spectrometer (Avantes) as detector, both connected to the cuvette holder at a 180° angle and both at a 90° angle with respect to the red laser irradiation direction. The filter holder between cuvette holder and detector was in a position without a filter (Figure S.V.3, item 8). Luminescence emission spectra were measured using the same detector but with the UV-Vis light source switched off. To visualize the spectrum

from 450 nm to 900 nm, while blocking the red excitation light, a Thorlabs NF-633 notch filter was used in the variable filter holder. All spectra were recorded with Avasoft software from Avantes and further processed with Microsoft Office Excel 2010 and Origin Pro software. Temperature dependent luminescence experiments were done with continuous irradiation and temperature ramping, except for phosphorescence measurements of compound **1** to prevent bleaching during the experiment. Instead, spectra were taken every 5 °C with 10 min thermal equilibration between temperature points.

6.5 References

[1] a) Q. Liu, W. Feng, T. Yang, T. Yi, F. Li, *Nat. Protocols* **2013**, *8*, 2033-2044; b) J.-H. Kim, J.-H. Kim, *J. Am. Chem. Soc.* **2012**, *134*, 17478-17481; c) P. Mahato, A. Monguzzi, N. Yanai, T. Yamada, N. Kimizuka, *Nat. Mater.* **2015**, *14*, 924-930.

[2] a) R. R. Islangulov, D. V. Kozlov, F. N. Castellano, *Chem. Commun.* **2005**, 3776-3778; b) S. Baluschev, T. Miteva, V. Yakutkin, G. Nelles, A. Yasuda, G. Wegner, *Phys. Rev. Lett.* **2006**, *97*, 143903.

[3] a) M. Majek, U. Faltermeier, B. Dick, R. Pérez-Ruiz, A. Jacobi von Wangelin, *Chem. Eur. J.* **2015**, *21*, 15496-15501; b) O. S. Kwon, J. H. Kim, J. K. Cho, J. H. Kim, *ACS Appl. Mater. Interfaces* **2015**, *7*, 318-325.

[4] a) A. Monguzzi, S. M. Borisov, J. Pedrini, I. Klimant, M. Salvalaggio, P. Biagini, F. Melchiorre, C. Lelii, F. Meinardi, *Adv. Funct. Mater.* **2015**, *25*, 5617-5624; b) A. Nattestad, C. Simpson, T. Clarke, R. W. MacQueen, Y. Y. Cheng, A. Trevitt, A. J. Mozer, P. Wagner, T. W. Schmidt, *Phys. Chem. Chem. Phys.* **2015**; c) S. P. Hill, T. Banerjee, T. Dilbeck, K. Hanson, *J. Phys. Chem. Lett.* **2015**, *6*, 4510-4517; d) A. Nattestad, Y. Y. Cheng, R. W. MacQueen, T. F. Schulze, F. W. Thompson, A. J. Mozer, B. Fückel, T. Khoury, M. J. Crossley, K. Lips, G. G. Wallace, T. W. Schmidt, *J. Phys. Chem. Lett.* **2013**, *4*, 2073-2078.

[5] a) S. H. C. Askes, M. Kloz, G. Bruylants, J. T. Kennis, S. Bonnet, *Phys. Chem. Chem. Phys.* **2015**, *17*, 27380-27390; b) S. H. C. Askes, A. Bahreman, S. Bonnet, *Angew. Chem., Int. Ed.* **2014**, *53*, 1029-1033.

[6] a) A. Nagai, J. B. Miller, P. Kos, S. Elkassih, H. Xiong, D. J. Siegwart, *ACS Biomater. Sci. Eng.* **2015**, *1*, 1206-1210; b) C. Wohnhaas, V. Mailänder, M. Dröge, M. A. Filatov, D. Busko, Y. Avlasevich, S. Baluschev, T. Miteva, K. Landfester, A. Turshatov, *Macromol. Biosci.* **2013**, *13*, 1422–1430; c) Q. Liu, B. Yin, T. Yang, Y. Yang, Z. Shen, P. Yao, F. Li, *J. Am. Chem. Soc.* **2013**, *135*, 5029-5037; d) O. S. Kwon, H. S. Song, J. Conde, H.-i. Kim, N. Artzi, J.-H. Kim, *ACS Nano* **2016**, *10*, 1512-1521.

[7] a) J. Zhou, Q. Liu, W. Feng, Y. Sun, F. Li, *Chem. Rev.* **2014**, *115*, 395-465; b) T. N. Singh-Rachford, F. N. Castellano, *Coord. Chem. Rev.* **2010**, *254*, 2560-2573.

[8] a) S. Hisamitsu, N. Yanai, N. Kimizuka, *Angew. Chem. Int. Ed.* **2015**, *54*, 11550-11554; b) S. H. Lee, D. C. Thévenaz, C. Weder, Y. C. Simon, *J. Polym. Sci., Part A: Polym. Chem.* **2015**, *53*, 1629-1639; c) P. Duan, N. Yanai, H. Nagatomi, N. Kimizuka, *J. Am. Chem. Soc.* **2015**, *137*, 1887-1894; d) P. Duan, N. Yanai, N. Kimizuka, *J. Am. Chem. Soc.* **2013**, *135*, 19056–19059; e) A. J. Svagan, D. Busko, Y. Avlasevich, G. Glasser, S. Baluschev, K. Landfester, *ACS Nano* **2014**, *8*, 8198-8207.

[9] a) J.-H. Kim, J.-H. Kim, *ACS Photonics* **2015**, *2*, 633-638; b) Z. Huang, X. Li, M. Mahboub, K. Hanson, V. Nichols, H. Le, M. L. Tang, C. J. Bardeen, *Nano Lett.* **2015**, *15*, 5552-5557.

[10] a) Y. C. Simon, C. Weder, *J. Mater. Chem.* **2012**, *22*, 20817-20830; b) A. Monguzzi, M. Mauri, A. Bianchi, M. K. Dibbanti, R. Simonutti, F. Meinardi, *J. Phys. Chem. C* **2016**, *120*, 2609-2614.

[11] T. N. Singh-Rachford, J. Lott, C. Weder, F. N. Castellano, *J. Am. Chem. Soc.* **2009**, *131*, 12007-12014.

[12] G. Massaro, J. Hernando, D. Ruiz-Molina, C. Roscini, L. Latterini, *Chem. Mater.* **2016**.

[13] D. Marsh, *Handbook of Lipid Bilayers*, 2nd ed., Taylor & Francis Group, LLC, Boca Raton, FL, USA, **2013**.
[14] a) M. Penconi, P. L. Gentili, G. Massaro, F. Elisei, F. Ortica, *Photochem. Photobiol. Sci.* **2014**, *13*, 48-61; b) S. H. C. Askes, N. Lopez Mora, R. Harkes, R. I. Koning, B. Koster, T. Schmidt, A. Kros, S. Bonnet, *Chem. Commun.* **2015**, *51*, 9137-9140.
[15] C.-H. Chang, H. Takeuchi, T. Ito, K. Machida, S.-i. Ohnishi, *J. Biochem.* **1981**, *90*, 997-1004.
[16] T. K. Khan, P. L.-G. Chong, *Biophys. J.* **2000**, *78*, 1390-1399.